

Desktop NMR spectroscopy for real-time monitoring of an acetalization reaction in comparison with gas chromatography and NMR at 9.4 T

Kawarpal Singh¹  · Ernesto Danieli¹ · Bernhard Blümich¹

Received: 11 July 2017 / Revised: 18 September 2017 / Accepted: 29 September 2017 / Published online: 13 October 2017
© Springer-Verlag GmbH Germany 2017

Abstract Monitoring of chemical reactions in real-time is in demand for process control. Different methods such as gas chromatography (GC), mass spectroscopy, infrared spectroscopy, and nuclear magnetic resonance (NMR) are used for that purpose. The current state-of-the-art compact NMR systems provide a useful method to employ with various reaction conditions for studying chemical reactions inside the fume hood at the chemical workplace. In the present study, an acetalization reaction was investigated with compact NMR spectroscopy in real-time. Acetalization is used for multistep synthesis of the variety of organic compounds to protect particular chemical groups. A compact 1 T NMR spectrometer with a permanent magnet was employed to monitor the acid catalyzed acetalization of the *p*-nitrobenzaldehyde with ethylene glycol. The concentrations of both reactant and product were followed by peak integrals in single-scan ¹H NMR spectra as a function of time. The reaction conditions were varied in terms of temperature, agitation speed, catalyst loading, and feed concentrations in order to determine the activation energy with the help of a pseudo-homogeneous kinetic model. For low molar ratios of aldehyde and glycol, the equilibrium conversions were lower than for the stoichiometric ratio. Increasing catalyst concentration leads to faster conversion. The data obtained with low-field NMR spectroscopy were compared with data from GC and NMR spectroscopy at 9.4 T

acquired in batch mode by extracting samples at regular time intervals. The reaction kinetics followed by either method agreed well. The activation energies for forward and backward reactions were determined by real-time monitoring with compact NMR at 1 T were 48 ± 5 and 60 ± 4 kJ/mol, respectively. The activation energies obtained with gas chromatography for forward and backward reactions were 48 ± 4 and 51 ± 4 kJ/mol. The equilibrium constant decreases with increasing temperature as expected for an exothermic reaction. The impact of dense sampling with online NMR and sparse sampling with GC was observed on the kinetic outcome using the same kinetic model.

Keywords Compact NMR spectroscopy · Reaction monitoring · Acetalization · Kinetic model · Gas chromatography · Activation energy · High-field NMR

Abbreviations

ID	One-dimensional
CDCl ₃	Deuterated chloroform
EG	Ethylene glycol
FID	Free induction decay
GC	Gas chromatography
mM	Millimolar
NMR	Nuclear magnetic resonance
ppm	Parts per million
PTFE	Polytetrafluoroethylene
RPM	Rotations per minute
RTD	Residence time distribution

Electronic supplementary material The online version of this article (<https://doi.org/10.1007/s00216-017-0686-y>) contains supplementary material, which is available to authorized users.

✉ Kawarpal Singh
Singh@itmc.rwth-aachen.de

¹ Institut für Technische Chemie und Makromolekulare Chemie, RWTH Aachen University, Worringerweg 1, 52074 Aachen, Germany

Introduction

Optimization of chemical processes is of central importance in process engineering. Efficiency, stability, information content,

economy, etc. are the parameters which are normally desired for choosing an analytical method. Depending upon the type of information required, different methods such as chromatography, mass spectrometry, calorimetry, gravimetric analysis, spectroscopy, etc. are used for chemical process engineering.

Nuclear magnetic resonance (NMR) is a unique analytical technique, because it is quantitative [1]. No calibration is required under correct acquisition conditions. This makes it particularly interesting for reaction monitoring. NMR spectroscopy is generally used for determining the structure, conformation, purity, percentage yield, and kinetic isotope ratio of the reaction products in synthetic as well as in natural product chemistry [2]. Usually, a chemical reaction can be monitored in three ways: (a) at-line, (b) batch wise, and (c) online. In at-line reaction monitoring, the chemical reaction proceeds inside the NMR tube as a batch following addition of the reaction components and mixing them by simply shaking the tube for a while. After insertion into the spectrometer, the reaction mixture needs to settle for some time to avoid convection before the NMR observation can begin. Spectra of the reaction mixture are then recorded in regular time intervals to follow the reaction progress. In batch mode reaction monitoring, the chemical reaction is conducted outside the analytical instrument such as the NMR spectrometer. Aliquots are taken from the reaction mixture in suitable time intervals and prepared as solutions for analysis in a laboratory, for which NMR spectrometers are normally distant from the chemical synthesis laboratory. In online monitoring, the chemical reaction is performed outside the magnet and the reaction mixture is flown continuously through the magnet using the suitable tubing at a desired flow rate. Spectra of the flowing mixture are recorded in regular time intervals depending upon the T_1 relaxation time of the slowly decaying component in the reaction mixture to obtain the spectrum under equilibrium conditions. Monitoring a reaction in batch mode has two disadvantages; one is the limitation of the time resolution by the rate of collecting aliquots, and the other is the need to quench the reaction in the aliquots. Quenching often demands particular solvents, reagents, and separation processes such as centrifugation. None of these applies to online monitoring as long as sensitivity and speed of measurement are compatible with the reaction. Special setups have been designed for reaction monitoring using high-field NMR spectroscopy in dedicated laboratories. These setups include rapid injection [3] and stopped flow operations [4] in order to transfer the reaction mixture quickly into the magnet. In recent years, reaction monitoring techniques have been developed by which a reaction mixture can be passed through conventional 5-mm-diameter sample tubes inside a superconducting magnet [5–7].

Today's state-of-the-art spectrometers provide superior sensitivity and resolution so that a wider range of chemical reactions can be studied. Until recently, all modern NMR spectrometers were equipped with superconducting magnets,

which enable high magnetic fields, for high sensitivity and high chemical-shift dispersion. Most of these magnets are too large and delicate to operate within an ordinary chemical synthesis laboratory. Moreover, they demand expert training for operation and maintenance, as well as the budget for cryogenic cooling. Apart from operational complexity, these large magnets necessitate long tubes to loop the reactant from the reactor through the magnet, which delay the time between reaction and measurement, and limit the time resolution by flow dispersion. As a partial solution to these problems, flow cells which are optimized to the flow regime and NMR relaxation times [8] can be used to obtain spectra with the best possible sensitivity and resolution. Nevertheless, due to the long time delay of the fluid looping through the magnet, the difference in reaction parameters for the reaction mixture inside the reactor and the reaction mixture inside the NMR magnet can impact the information derived from the NMR spectra. Consequently, mostly slow reactions are monitored at ambient conditions with such instruments [9]. Multiphase reactions present a particular challenge, because they need to be continuously agitated to remove the mass transfer resistance. While there is no general solution to these issues today, small and compact NMR spectrometers with permanent magnets are maintenance free, can be set up in the chemistry laboratory, and require much shorter feed lines [10]. Despite their lower field strength, they give sufficient sensitivity and spectral dispersion and bear promise to alleviate many of the challenges mentioned above.

With desktop NMR spectrometers, the delay from sample preparation to spectrum analysis can be shortened to a few minutes when setting up the spectrometer in the chemistry laboratory. As an alternative to thin-layer and gas chromatography, compact NMR spectroscopy [11] can serve to monitor chemical reactions in a simple and accurate way [12, 13], especially when the initial reaction rates are critical. Because the measurement happens in real time, the NMR parameters can be employed to control the reaction conditions and kinetics.

Gas chromatography (GC) is a very stable, sensitive, and standard method used in process engineering where very few microliters of the sample are required to perform the measurement [14]. Helium or nitrogen need to be used as a carrier gas for the mobile phase. The stationary phase has to be chosen to suit the particular samples in order to avoid detrimental chemical interactions with the sample. The measurement times of the GC can be long depending upon the retention time of the reactants, products, and intermediates. On the other hand, the chemical shift range for ^1H nuclei lies within the range of 0 to 12 ppm which is usually sufficient for detecting the ^1H nuclei from reactants, products, and intermediates using ^1H NMR spectroscopy. The sensitivity of table top NMR spectrometers suffices to acquire a ^1H NMR spectrum in a single shot in 15 s. Online NMR provides densely sampled data compared to GC

which provides sparsely sampled data, therefore densely sampled data can provide more reliable kinetic information than sparsely sampled data. NMR is a calibration-free method because of the linearity between the absolute signal area to the number of spins and sample concentration. Compact NMR systems do not require any helium filling. In terms of stability and sensitivity, GC measurements are similarly stable and accurate but more sensitive than compact NMR measurements.

Acetalization reactions are used in a variety of chemical syntheses to protect functional groups in the chemistry of carbonyl compounds and intermediate products [15]. Aldehydes are unstable in alkaline conditions and the carbonyl groups need to be protected against the reduction from nucleophilic groups. Carbonyl compounds can be converted via acetalization into many other functional groups, such as acyclic and cyclic acetals (1, 3-dioxolanes), which serve as intermediates in chemical and biochemical syntheses [16]. Acetalization reactions produce major intermediates in the polymer, fragrance, and pharmaceutical industries. Many biologically active compounds, which have aryl, alkyl, imidazole, triazole, pyrazole, benzimidazole, benzotriazole, oxypurine, pyrimidinyl, and naphthyl groups linked to a 1, 3-dioxolane ring at positions 2, 4, or 5 are important to the pharmaceutical industry, because of their use in antifungal, antibacterial, antineoplastic, and antiviral drugs [17]. Depending on the structure of the substrate molecule, each compound exhibits different properties. Acetals are used for increasing the cetane number of fuel, for example as diesel additives, in order to improve the combustion by shortening the ignition delay [18]. Moreover, 1,3-dioxolanes are used in electrolytes of batteries [19]. Different methods and strategies have been followed to produce 1,3-dioxolanes and monitor their syntheses [20, 21]. 1,3-Dioxolanes (cyclic acetals) are usually formed from benzaldehyde or other aromatic aldehydes by reaction with ethylene glycol in the presence of acid catalysts [22]. This path involves a cyclic ring formation, which favors formation of the product rather than return to the reactant.

Reliable kinetic and thermodynamic data are available for acetalization reactions, studied with gas chromatography [23, 24]. This work reports the kinetics of an acetalization reaction monitored with a compact NMR spectrometer at 1 T in comparison with gas chromatography and NMR at 9.4 T. An efficient and easy way is presented to monitor the acetalization reaction and analyzing it by controlling different reaction parameters, such as temperature, catalyst concentration, initial reactant concentrations, and agitation speed. The reaction kinetics, order, equilibrium conversion, equilibrium conditions, and activation energy are interpreted in terms of a pseudo-homogeneous kinetic model. The results obtained are compared with results from gas chromatography and NMR spectroscopy at 9.4 in batch mode, showing very good agreement.

Materials

Ethylene glycol, *p*-nitrobenzaldehyde, *p*-toluenesulphonic acid, sodium bicarbonate, and sodium chloride were purchased from Sigma Aldrich Chemie GmbH, Steinheim, Germany. Toluene was purchased from Th. Geyer GmbH and Co. KG, Renningen, Germany. Acetone and isopropanol were obtained from the chemical shop of RWTH Aachen University. 2-(4-Nitrophenyl)-1, 3-dioxolane was synthesized by performing the acetalization reaction in the laboratory at ITMC. The synthetic procedure is given in the [supplementary information](#).

Experimental

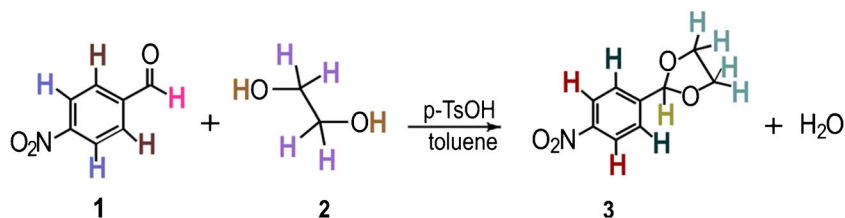
Acetalization reaction

The acid-catalyzed acetalization of *p*-nitrobenzaldehyde (**1**) with ethylene glycol (**2**) (Scheme 1) was studied in the temperature range from 333 to 370 K for the synthesis of 2-(4-nitrophenyl)-1, 3-dioxolane (**3**). In each experiment, *p*-nitrobenzaldehyde (0.55 mol L⁻¹) and *p*-toluene sulfonic acid monohydrate 0.2 wt% were dissolved in 150 ml toluene (solvent) contained in a 500 ml three-necked round-bottom flask. After proper mixing, ethylene glycol (0.55 mol L⁻¹) was added with a syringe. The solution was refluxed with a condenser. The reaction mixture was stirred at a rate of 200 RPM with the mechanical stirrer to avoid mass transfer effects due to the viscous behavior of ethylene glycol at room temperature and at lower stirring speeds. During each measurement, 2 ml of sample were taken with a syringe after different time intervals at 2, 5, 10, 15, 25, 35, 45, 60, 90, 100, 150, 210, 270, 360 min and so on depending upon the reaction time. Each sample was quenched with 4 ml of saturated solution of sodium bicarbonate. The resultant solution was shaken for a while and then added to the separating funnel. In the separating funnel, saturated solution of sodium chloride (4 ml) was added and then shaken again. After some time, the solution separates into two phases. The lower layer contains the unreacted ethylene glycol and water, and upper layer contains toluene, unreacted reactant (*p*-nitrobenzaldehyde), and product (2-(4-nitrophenyl)-1, 3-dioxolane). The lower layer was taken away and the upper layer was used for the batch analysis with gas chromatography and NMR spectroscopy at 9.4 T.

Online NMR setup for compact NMR spectroscopy

A compact NMR spectrometer (Magritek Spinsolve) was employed for studying the acetalization of the *p*-nitrobenzaldehyde with ethylene glycol to yield 2-(4-nitrophenyl)-1, 3-dioxolane at different temperatures ranging from 333 to 370 K (Fig. S1).

Scheme 1 Overall reaction between *p*-nitrobenzaldehyde and ethylene glycol



Flow setup and temperature

The reaction mixture was circulated through the NMR magnet (Fig. 1a) with a specially designed flow cell of 5 mm outer diameter in the center near the sensitive volume and 1 mm outer diameter away from the center (Fig. 1b). The flow cell was connected to PTFE (polytetrafluoroethylene) tubing of 1/16" OD and 1 mm ID. The tubing was inserted into the reactor and connected to a peristaltic pump forming a closed loop through the NMR spectrometer. The reactants which are not completely miscible when present in the reactor require rigorous stirring. The rigorous stirring cannot be performed using at-line NMR procedures, which are usually employed with high-field NMR. Therefore, online NMR involving the reactor outside the magnet enables complete dispersion and mixing of the reaction mixture. The reaction mixture was flowing inside the magnet at the magnet temperature of 301.5 K, while the reactor temperature was set at the desired temperature range with the aid of heater. The temperature fluctuation in the reactor was 0.9 K due to fluctuation in the temperature of the heater from the surroundings. The reaction mixture was cooled down to the temperature of the magnet by making 2 cm diameter coils of the PTFE tubing and immersing them in cold water. Because the reaction time was long compared to the time required for the measurement after lowering the temperature, it can be assumed that the reaction kinetics are hardly affected. The data obtained from gas

chromatography and NMR spectroscopy at 9.4 T validate this assumption. The reaction mixture was pumped with the aid of a three-channel peristaltic pump (ISMATEC® Relgo) at a flow rate of 0.65 ml/min. After each reaction, the tubing was washed with acetone to remove residual reaction mixture adhering to the walls. Subsequently, the tubes were rinsed with toluene to ensure the removal of any droplets of acetone.

Delay times

The time between a change in the composition of the reaction mixture in the reactor and corresponding change in the signal amplitude of the NMR signal is the important parameter that needs consideration for monitoring the reaction kinetics. The time which the reaction mixture takes from the reactor to the active region is the transfer time denoted by t_{trans} . The reaction mixture fills the active volume starting from its tracer concentration to the stationary value. The time it takes is denoted by t_{delay} . The difference between t_{trans} and t_{delay} is called dwell time t_{dwell} [25]. For obtaining the reliable NMR data, it is required to completely replace the solution in the NMR probe with the fresh sample. The transfer time t_{trans} was determined to be 66.4 s. The delay time of 126.5 s and dwell time of 60.5 s was used for the present reaction which is very short compared to the reaction time.

Non-ideal flow of the sample from the chemical reactor to the sensitive volume of the NMR results from back mixing, stagnant regions, and spreading of the sample at different positions during the flow (Fig. S2). This behavior of the liquid in the pipes is described by the residence time distribution (RTD) profile. The RTD profile was determined at 0.65 ml/min flow rate using the step tracer experiment with acetone and isopropanol solution where 3% acetone solution in isopropanol was replaced with pure isopropanol to see the concentration step produced in the reactor and the NMR signal. The mean residence time \bar{t}_{res} was determined to be 96.6 s. The t_{dwell} can also be determined from the relation of t_{res} and t_{dwell} following Eq. 1.

$$\bar{t}_{\text{res}} = t_{\text{trans}} + t_{\text{dwell}}/2 \quad (1)$$

From the knowledge of the RTD function, the time-dependent concentration changes in the reactor $S_{\text{react}}(t)$

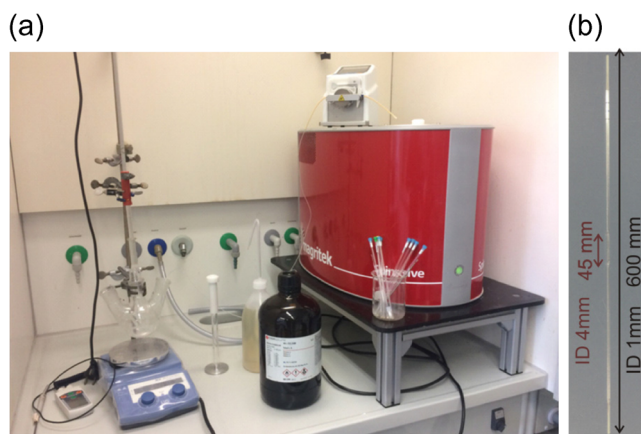


Fig. 1 Experimental setup. **a** Compact 1 T NMR spectrometer and reaction set-up inside the fume hood. **b** Flow cell to pass the reaction mixture through the magnet

can be reconstructed from the NMR signal $S_{\text{NMR}}(t)$ by following Eq. 2.

$$S_{\text{react}}(t) = S_{\text{NMR}}(t + \bar{t}_{\text{res}}) \quad (2)$$

The data lost before the first measurement within $\bar{t}_{\text{res}} = 2$ min were extrapolated from seven measurements with an accuracy of $\pm 2\%$.

Polarization length

The pre-polarization volume of the reaction mixture needs to be studied for the reaction optimization. Pre-polarization volume is the volume of the reaction mixture inside the magnet which should be pre-polarized enough to monitor the reaction under equilibrium conditions depending upon the longitudinal relaxation times of the components of the reaction mixture. The variation of signal amplitude of the mixture of *p*-nitrobenzaldehyde and 2-(4-nitrophenyl)-1, 3-dioxolane in toluene was studied with different flow rates. The T_1 relaxation times of the different components of the reaction mixture were evaluated (Figs. S3 and S4). The pre-polarization length of 170 mm was determined by simulating Eq. 3 [26].

$$\frac{S}{S_0} = 1 - \exp\left(-\frac{L_{\text{pol}}}{\bar{v}T_1}\right) \quad (3)$$

S_0 is the signal amplitude under equilibrium conditions when ($t_r \rightarrow \infty$, $V \rightarrow 0$), i.e., at longer pulse repetition time and at zero flow rate. The flow rate under equilibrium conditions was 0.65 ml/min under the maximum T_1 time of 3.3 s which belongs to 1,3-dioxo protons in the 2-(4-nitrophenyl)-1, 3-dioxolane (Fig. S5). The pre-polarization length L_{pol} was determined from the change in signal amplitude of the $-\text{CH}_3$ isopropanol with flow rate (Fig. S6).

Shim procedure and shimming stability

Protonated solvent with 10 wt% of water in D_2O was used as shimming sample to shim the spectrometer with the automatic shimming procedure given in the spectrometer software. The line width observed after shimming was 0.5 Hz. When used every day, it takes 2.5 min to shim the magnet with the low-order shims. When used only occasionally, shimming all orders may take 40 min. Shimming can also be performed during the reaction on representative large peaks in the reaction mixture. The B_0 field is stabilized by an external lock together with the software lock which adjusts the ppm scale following the field drift. The shim was stable during all the reactions performed. No drift was observed during either experiment. The system was monitored by continuously flowing methanol for 24 h to see the drift in the field and change in the signal amplitude. The magnetic field B_0 was stable enough to realize

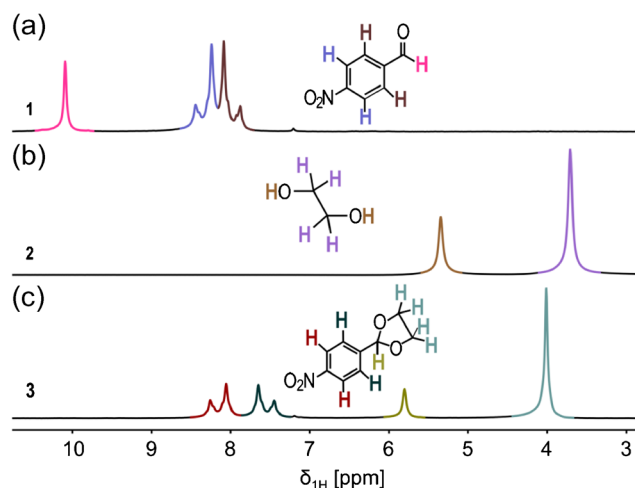


Fig. 2 1D ^1H NMR spectra of pure components of the acetalization reaction at 1 T. **a** *para*-Nitrobenzaldehyde (1). **b** Ethylene glycol (2). **c** 2-(4-nitrophenyl)-1, 3-dioxolane (3)

acquisition times of several hours without substantial change in the signal amplitude (Fig. S7).

Data acquisition

A single-scan free induction decay (FID) was measured every 15 s from the beginning to the end of the reaction using a 43.2 MHz (1 T) Magritek Spinsolve NMR spectrometer. Each spectrum used a $\pi/2$ excitation pulse of 7 μs , an acquisition time of 6.6 s, an acquisition bandwidth of 5 kHz, and dwell time of 200 μs with 32,768 data points.

Data processing

The original FID data were recorded and saved by the spectrometer software. The saved data were processed and

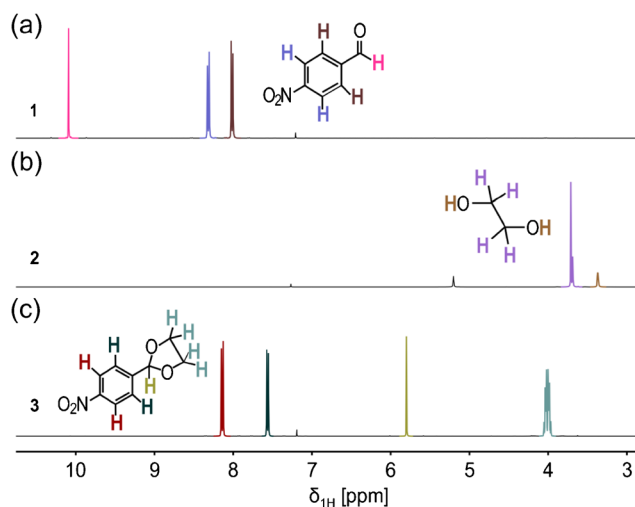
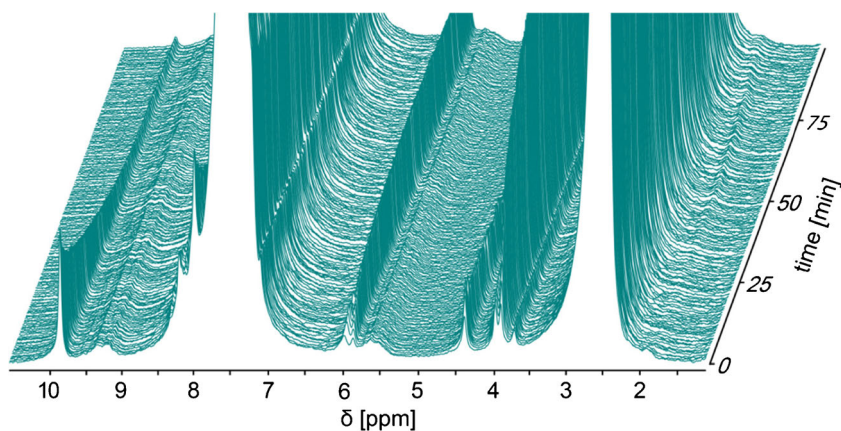


Fig. 3 1D ^1H NMR spectra of pure components of the acetalization reaction at 9.4 T. **a** *para*-Nitrobenzaldehyde (1). **b** Ethylene glycol (2). **c** 2-(4-nitrophenyl)-1, 3-dioxolane (3)

Fig. 4 Stack plot of spectra acquired during 100 min of the reaction of *p*-nitrobenzaldehyde (0.55 mol L^{-1}) and *p*-toluene sulfonic acid monohydrate 0.2 wt% dissolved in toluene (solvent) and ethylene glycol (0.55 mol L^{-1}) at a temperature of 370 K with an agitation speed of 200 RPM



analyzed with MestreNova® (Mestrelab Research S. L., Santiago de compostela Spain) 11.0 software. All the spectra were aligned using the reference alignment tool in MNova. The $-\text{CH}_3$ peak of toluene at 2.3 ppm was used as a reference to align the NMR spectra. The integration range was set by considering the line width and neighboring peaks of the desired signal using sum method. The exponential apodization of 0.6 Hz was used to increase the resolution. The values obtained for the signal amplitude as a function of the reaction time were transferred to Origin® 9.0 to plot the graphs. The different values of the reaction rate constants for real-time NMR and gas chromatography were evaluated with the Runge-Kutta fourth-order method using Matlab.

High-field NMR spectroscopy at 9.4 T

During the course of the reaction, aliquots of 2 ml were extracted with a syringe at different time intervals. The samples obtained were quenched with saturated solution of sodium bicarbonate (NaHCO_3). The resultant solution was shaken for 5 min before transferring to the separating funnel for separating the aqueous and organic layers. The solution was washed with brine. The lower aqueous layer contained ethylene glycol and water, and upper layer contained unreacted *p*-

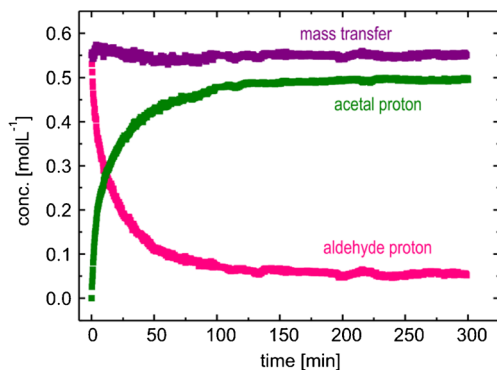


Fig. 5 Variation of ^1H NMR peak integrals with time at 370 K for 300 min. The reactant signal of the aldehyde proton decreases while the product signal of the acetal proton increases

nitrobenzaldehyde and 1,3-dioxolane. The lower layer was removed and the upper layer was used for quantification. Each NMR sample was prepared in a 5 mm NMR tube by adding 0.05 ml of sample into 0.5 ml of deuterated chloroform. Each sample was measured at 9.4 T with 16 scans in 1.5 min.

The calibration samples were prepared with knowledge of limits of detection and quantification at 1 (Fig. S8) and 9.4 T (Fig. S9) with known concentrations of *p*-nitrobenzaldehyde and 1,3-dioxolane. Data for the calibration curves are given in the [supplementary information](#).

Gas chromatography

The same samples obtained by quenching the reaction mixture were used for the gas chromatographic measurements with high-purity helium at a flow rate of 1.5 ml/min. A ThermoScientific TRACE 1 gas chromatograph with flame ionization detector (FID) was used with CP-Sil-Pona column capillary of 50 m length. The retention time of *p*-nitrobenzaldehyde and 1,3-dioxolane were 12.6 and 18.1 min, respectively.

The calibration samples were prepared with known concentrations of *p*-nitrobenzaldehyde and 1,3-dioxolane with given concentration of each component and area (Fig. S10). The

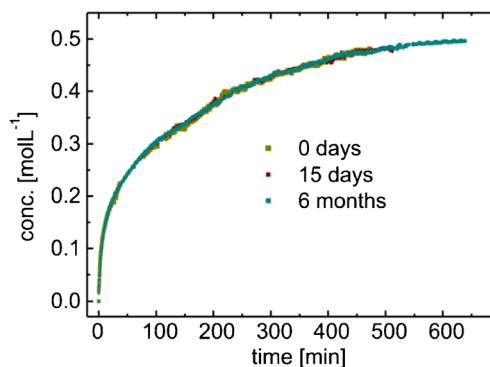


Fig. 6 Repeatability measurements after intervals of days and months for the acetalization reaction at 333 K

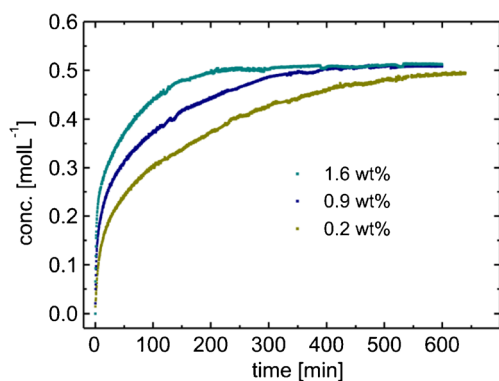


Fig. 7 Effect of catalyst loading on the concentration of the product in terms of the concentration of the acetal proton versus the reaction time

details of calibration curves are given in the [supplementary information](#).

Results and discussion

1D ^1H NMR spectra at 1 and 9.4 T for the acetalization

In the acetalization reaction, the 1D ^1H NMR spectra of *p*-nitrobenzaldehyde (**1**) at 1 (Fig. 2a) and 9.4 T (Fig. 3a) showed the peaks of the aldehyde proton at 10.4 ppm. The two aromatic protons close to the $-\text{NO}_2$ group showed a multiplet centered at 8.3 ppm and the other two protons close to the $-\text{CHO}$ group appeared at 8 ppm (Fig. 2). 1D ^1H NMR spectrum of ethylene glycol (**2**) showed a single peak corresponding to the hydroxyl proton at 5.4 ppm and a single peak for the $-\text{CH}_2-\text{CH}_2-$ group at 3.7 ppm at 1 (Fig. 2b) and 9.4 T (Fig. 3b). The 1D ^1H NMR spectrum of 2-(4-nitrophenyl)-1,3-dioxolane (**3**) showed a single peak corresponding to the acetal proton at 5.8 ppm. A single peak corresponding to the four protons in the 1,3-dioxo group appeared at 4 ppm at 1 T (Fig. 2a) while a multiplet centered at 4 ppm was observed at 9.4 T (Fig. 3a). The two aromatic protons adjacent to the 1,3-dioxo group appeared at 7.56 ppm and the two protons near to the $-\text{NO}_2$ group at 8.14 ppm. The 1D ^1H NMR spectra at 1 and 9.4 T are in

complete agreement with each other. Peaks corresponding to different chemical groups can be easily distinguished at 1 T in spite of low field strength.

Real-time monitoring of the acetalization reaction with 1D ^1H NMR spectroscopy

The concentrations of reacting components in the mixture vary as the reaction progresses. This variation is followed in a stack of spectra (Fig. 4), where each spectrum was acquired in 15 s one after the other. Corresponding to the low-field NMR spectra of the reactants and products described in the “1D ^1H NMR spectra at 1 and 9.4 T for the acetalization” section, the real-time NMR data reveal that the peak integrals (concentration) of the aldehyde proton in the *p*-nitrobenzaldehyde (reactant) at 10.4 ppm decrease, and the peak integrals of the 1,3-dioxo and acetal protons near 4 and 5.8 ppm, respectively, increase with the formation of the product (Fig. 5). Their time dependence can be modeled to extract the parameters describing the reaction kinetics.

Toluene is used as a solvent whose concentration is 19 times higher than the other analytes. Reactions, which proceed in protonated solvents at high concentrations, are very difficult to monitor at low field due to low chemical shift resolution. But because the lines are narrow due to the excellent field homogeneity of the instrument, the changing peak integrals of the prominent acetal and carbonyl protons can readily be followed in the stack of spectra acquired during the course of the reaction as a function of the reaction time in addition to the slight changes in chemical shift of the peaks corresponding to the aromatic protons in the *p*-nitrobenzaldehyde and 2-(4-nitrophenyl)-1,3-dioxolane near 8 ppm which are occurring during the reaction.

Repeatability: effect of system stability

Stability of the system is essential for quality control in process engineering applications. The acetalization reaction was repeated at 333 K in the interval of days and months in order

Fig. 8 Variation of the reaction rate for different molar ratios of the reactants. **a** The ethylene glycol concentration was varied and the *p*-nitrobenzaldehyde concentration was kept constant. **b** The ethylene glycol concentration was kept constant and the *p*-nitrobenzaldehyde concentration was varied

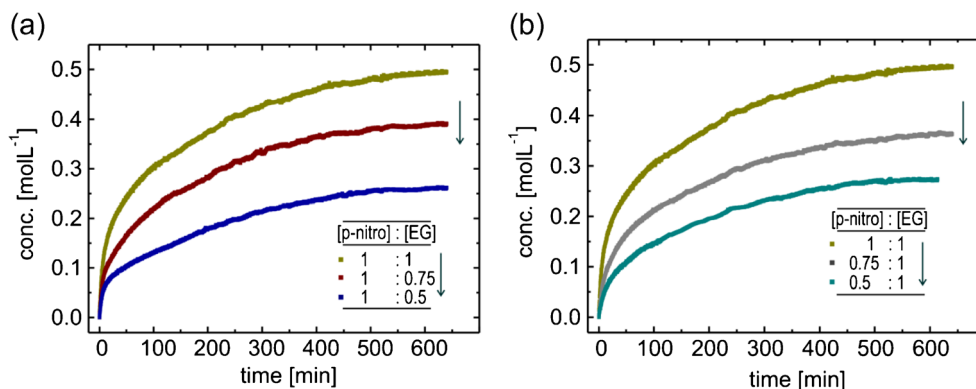
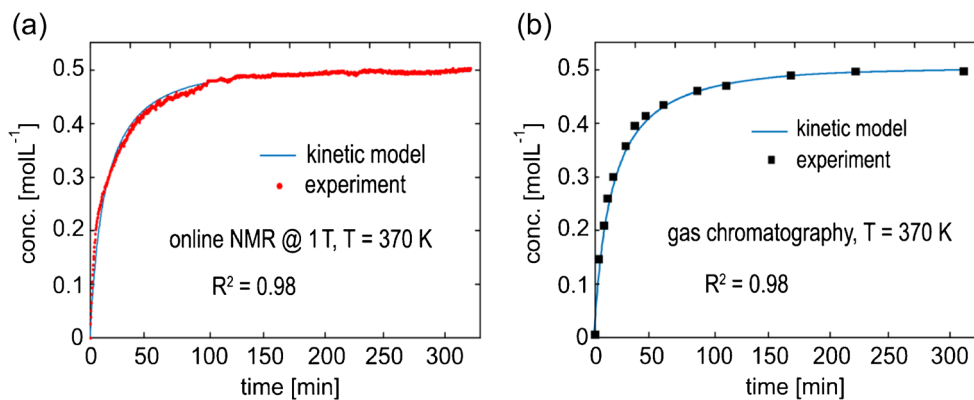


Fig. 9 Kinetic model fitted with the experimental results calculated by following the concentration of the acetal proton of the 2-(4-nitrophenyl)-1,3-dioxolane (product). **a** Online NMR at 1 T. **b** Gas chromatography



to see the impact of system stability on reaction kinetics. The NMR spectrometer was shimmed every time before starting the reaction using the automatic shim routine given in the instrument software. The system showed excellent repeatability (Fig. 6).

Mass transfer resistance: effect of stirring speed

Low stirring speeds and viscous mixtures are most unfavorable candidates responsible for resistance to external mass transfer. Vigorous stirring was necessary to achieve a homogeneous mixture of the reaction components which could not be obtained at lower stirring speeds because of the viscosity of ethylene glycol. Also, elimination of mass transfer resistance is important for studying the reaction rate in order to ensure that the rate of the reaction is not influenced by energy required for transfer of molecules from one phase to the other. The reaction mixture was stirred mechanically at rates varying from 200 to 400 RPM at a reaction temperature of 333 K with 0.2 wt% of *p*-toluene sulphonic acid as catalyst. The reaction rate turned out to be essentially independent of the stirring speed above 200 RPM. After ensuring the absence of mass transfer resistance, all experiments were carried out at 200 RPM (Fig. S11).

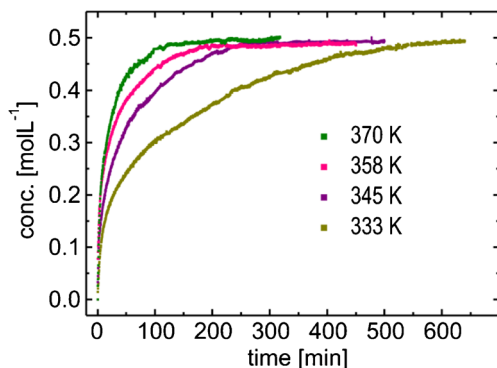


Fig. 10 Evolution of the acetal protons of product peaks with time for temperatures ranging from 333 to 370 K at 200 RPM agitation speed and 0.2 wt% catalyst concentration

Effect of catalyst loading

The amount of catalyst is an important parameter which influences the conversion rate of the reaction. The impact of catalyst concentration was studied by varying the amount of *p*-toluene sulphonic acid (catalyst) from 0.2 to 1.6 wt%. With increasing amount of catalyst, the reaction rate increases. The more active catalyst sites are available to assist the protonation of the carbonyl oxygen of *p*-nitrobenzaldehyde, the faster is the reaction. Because the protonation of the carbonyl carbon is controlled by the proton in the *p*-toluene sulphonic acid catalyst, the concentration of the 1,3-dioxo group of the product increases with increasing catalyst amount at a particular time (Fig. 7). The higher the catalyst loading, the higher is the rate of conversion.

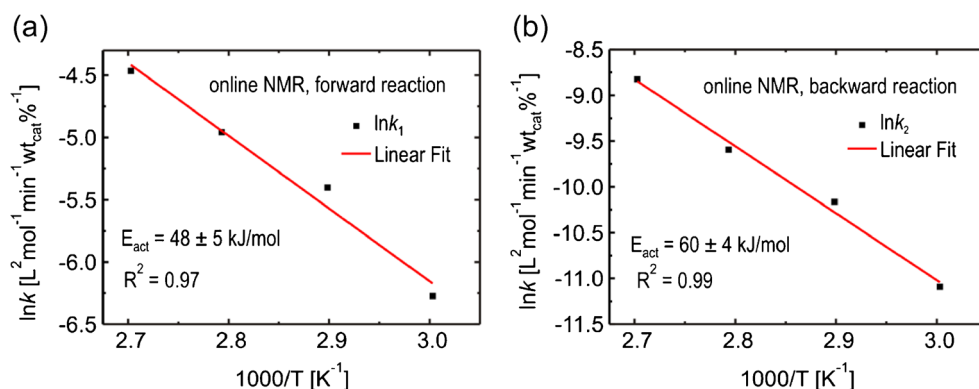
Effect of feed composition

The impact of the reactant concentrations on the reaction kinetics was studied by varying the ratios of the initial concentrations of *p*-nitrobenzaldehyde and ethylene glycol as 0.5:1, 0.75:1, and 1:1 as well as 1:0.5, 1:0.75, and 1:1. The reaction rate decreases as the concentrations deviate from the stoichiometric ratio of the reactants (Fig. 8). As a result, the equilibrium conversion decreases from 90 to 65.6 to 49.4% for decreasing the initial concentration of *p*-nitrobenzaldehyde while keeping the concentration of ethylene glycol constant equal to its stoichiometric concentration. Similarly, the equilibrium conversion decreases

Table 1 Rate constants for the reaction at temperatures ranging from 333 to 370 K using real-time NMR at 1 T

T [K]	$k_1 \times 10^{-3}$	95% confidence interval $\times 10^{-3}$	$k_2 \times 10^{-5}$	95% confidence interval $\times 10^{-6}$	R^2
333	1.89	[1.86, 1.91]	1.52	[1.51, 1.55]	0.9576
345	4.51	[4.37, 4.56]	3.86	[2.64, 3.96]	0.9718
358	7.04	[6.83, 7.17]	6.81	[5.15, 7.10]	0.9461
370	11.5	[11.2, 11.8]	1.47	[13.8, 15.0]	0.9846

Fig. 11 Arrhenius plots of the rate constants of the forward (a) and backward (b) reactions using online NMR at 1 T from which the activation energies were determined



from 90 to 70.9 to 47.4% when varying the initial concentration of ethylene glycol while keeping the initial concentration of *p*-nitrobenzaldehyde constant to stoichiometric concentration.

Modeling of the kinetic data

After ensuring the absence of mass transfer resistance, a kinetic model [27, 28] can readily be developed to extract the reaction rate constants from which the activation energy can be estimated by fitting model expressions to the time-dependent concentration data of the acetal protons present in the 2-(4-nitrophenyl)-1,3-dioxolane product (Fig. 9). From the data obtained by varying the temperature between 333 and 370 K, the activation energy of the reaction was estimated.

A pseudo-homogeneous kinetic model was used for obtaining the rate constants. The overall reaction between *p*-nitrobenzaldehyde ($C_7H_5O_3N$) and ethylene glycol (EG) in the presence of toluene as a solvent and *p*-toluene sulphonic acid as a catalyst (Scheme 1) yields 2-(4-nitrophenyl)-1,3-dioxolane (DIOX) and water (H_2O). Considering the time-dependent reactant concentrations $[C_7H_5O_3N]$ and $[EG]$, and the initial product concentrations

$$[DIOX]_0 = 0 = [H_2O]_0 \quad (4)$$

and the formation rate of the dioxolane product is written as

$$\frac{d[DIOX]}{dt} = wk_1[EG][C_7H_5O_3N] - wk_2[DIOX][H_2O], \quad (5)$$

Table 2 Rate constants for the reaction at temperatures ranging from 333 to 370 K using gas chromatography

T [K]	$k_1 \times 10^{-3}$	95% confidence interval $\times 10^{-3}$	$k_2 \times 10^{-5}$	95% confidence interval $\times 10^{-5}$	R^2
333	1.86	[1.82, 1.99]	1.38	[1.30, 1.47]	0.9915
345	4.10	[4.06, 4.13]	3.19	[2.73, 3.27]	0.9873
358	6.84	[6.71, 6.88]	5.13	[4.45, 5.45]	0.9803
370	10.7	[10.6, 10.8]	9.33	[8.24, 9.41]	0.9832

where $[i]$ is the concentration of the compound “*i*” in mol L^{-1} , w is the catalyst concentration in $\text{wt}\%_{\text{cat}}^{-1}$, and k_1 and k_2 are the reaction rate constants for the forward and the backward reactions in $\text{L}^2 \text{mol}^{-1} \text{min}^{-1} \text{wt}\%_{\text{cat}}^{-1}$. In the absence of side reactions, the concentrations of the other species are calculated by mass balance as

$$[EG] = [EG]_0 - [DIOX], \quad (6)$$

$$[C_7H_5O_3N] = [C_7H_5O_3N]_0 - [DIOX], \quad (7)$$

$$[H_2O] = [DIOX]. \quad (8)$$

The differential Eq. (5) was solved by fourth-order Runge-Kutta integration along with the initial conditions (4) and the mass balances (6, 7, and 8) using MATLAB.

The validity of the mass balance was verified by integrating the peaks of both reactants and products and forming the sum, which remained constant during the whole course of the reaction. The rate constants were determined by minimizing the sum of the square of the difference between the experimental and predicted concentrations. The 95% confidence intervals for the rate constants of each reaction were calculated from 1000 iterations to estimate the variation in the reaction kinetics following a Monte-Carlo approach.

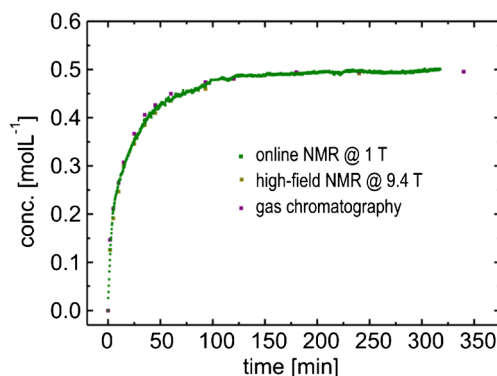
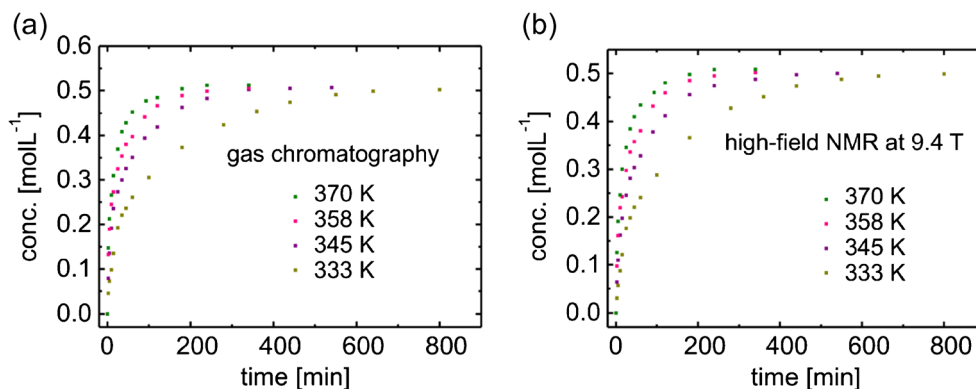


Fig. 12 Comparison of online NMR at 1 T, batch NMR at 9.4 T, and gas chromatography for the acetalization reaction at 370 K

Fig. 13 Evolution of the 1, 3-dioxolane product peaks with time for temperatures ranging from 333 to 370 K at 200 RPM agitation speed and 0.2 wt% catalyst concentration. **a** Gas chromatography. **b** High-field NMR at 9.4 T



Effect of temperature: NMR spectroscopy at 1 T

To determine the activation energies of the forward and backward reactions, the reaction kinetics were studied at temperatures of 333, 345, 358, and 370 K using the stoichiometric feed ratio. The reaction rates for both forward and backward reactions increase with increasing temperature. It is observed here that the reaction rate increases with increasing temperature (Fig. 10) as expected, but the final equilibrium conversion is independent of temperature. This observation was associated to heat effects in the reaction. Guemez et al. [23], Agirre et al. [27], and Silva et al. [28] have observed similar behavior in the same acetalization studies. This effect implies that the whole process has very low heat effects. According to the standard heat of formation, the acetalization reactions are exothermic [23, 27, 28] including the one in the present study. Nevertheless, it was observed that the heat of mixing between different reactants aldehyde and glycerol and water (product) is positive and the enthalpy of mixing between water and the formed acetal (product) is also positive showing endothermic behavior. The increase in temperature decreases the equilibrium constant of the reaction which revealed the exothermic behavior of the reaction (Table 1). The activation energies of the reaction retrieved by real-time monitoring for the forward and backward reactions turns out to be 48 ± 5 and 60 ± 4 kJ/mol, respectively (Fig. 11).

Gas chromatography and high-field NMR at 9.4 T

Each reaction was followed simultaneously by real-time monitoring with compact NMR at 1 T and batch monitoring with gas chromatography and high-field NMR at 9.4 T by extracting the samples after regular time intervals. The samples obtained were quenched and the organic layer was separated from the aqueous layer. The results obtained with gas chromatography (Table 2) and high-field NMR confirm the reaction kinetics obtained with the compact NMR at 370 K (Fig. 12) and at other temperatures also (Fig. 13). The activation energies obtained with gas chromatography for forward and backward reactions were 48 ± 4 and 51 ± 4 kJ/mol (Fig. S12). Each point in the

online-NMR measurement was obtained in 15-s intervals while for GC, the points were obtained in irregular intervals from 5 min to several hours. Therefore, the data points sampled with NMR (~ 1200) are much denser than those acquired with GC (~ 15) and provide more reliable kinetic information than sparsely sampled data. The higher sampling density is particularly important in the beginning of the reaction when concentrations change rapidly. The rate constants evaluated by minimizing the sum of square of the difference between experimental and predicted concentrations are more accurate because the error minimization is more reliable for a large number of data points than a low number of data points.

Conclusion

Real-time reaction monitoring by NMR spectroscopy is simplified with compact NMR spectrometers that can be operated on the laboratory bench. By example of an acetalization reaction, it is shown that the effects of parameters like temperature, feed composition, catalyst loading, and agitation speed can be directly monitored in terms of time-dependent reactant and product concentrations with the conclusion, that desktop NMR spectroscopy is an interesting tool to monitor, model, and optimize chemical reactions. For the studied acetalization reaction, the time-dependent concentrations of the various groups involved during the reaction were followed in order to estimate the equilibrium conversion in the acetalization reaction. This knowledge is particularly important for optimizing multistep syntheses. Real-time monitoring serves this purpose and there is no need to extract the reaction mixture, quench it, and then monitor the concentration of the chemical constituents involved with off-line gas chromatography and high-field NMR methods, which require additional preparation steps such as quenching, phase separation, dissolution, or centrifugation. Moreover, no deuterated solvents were needed for the NMR measurements due to the external lock in the spectrometer, and the magnet remained shimmed without field drift throughout an entire observation period of over 2 h. Deuterated solvents can also give rise to kinetic isotope effects

which would lead to changes in reaction kinetics. Gas chromatographic measurements are time consuming due to longer retention times of the chemical species involved in the reaction both reference methods need cryogenic coolants.

The data from the three methods showed excellent agreement. The experiment at 333 K was repeated three times over the duration of 15 days and 6 months in order to see the repeatability of the reaction and reproducibility of the instrument. No variation of instrument performance could be detected. The results agreed excellently well. The activation energies for forward and backward reactions that were determined by real-time monitoring were 48 ± 5 and 60 ± 4 kJ/mol, respectively. The activation energies obtained with gas chromatography for forward and backward reactions were 48 ± 4 and 51 ± 4 kJ/mol. The kinetic parameters derived from densely sampled data and sparsely sampled data showed differences in the rate constants. The data with large number of points provide a more reliable kinetic model than the data with few points. The equilibrium constant decreases with increasing temperature as expected for an exothermic reaction. Despite the low resolution and sensitivity, compact NMR has proven to be a reliable tool for monitoring chemical reactions in process engineering applications as accurate as other standard methods.

Acknowledgements The authors gratefully acknowledge financial support from Deutsche Forschungsgemeinschaft (DFG Gerätezentrum Pro2NMR) by a joint instrumental NMR facility BL 231/46-1 of RWTH Aachen University and KIT Karlsruhe. We are also thankful to GC department of ITMC especially to Elke Biener, Hannelore Eschmann, and Heike Boltz for providing the measurement time and data for the GC samples. Moreover we thank Sharoff Pon Kumar for helping in providing the MATLAB codes for running the Runge-Kutta method and optimizing the kinetic rate constants.

Compliance with ethical standards

Conflict of interest Bernhard Blümich is on the board of directors of Magritek Ltd.

References

- Ernst R, Bodenhausen G, Wokaun A. Principles of nuclear magnetic resonance in one and two dimensions. Oxford: Clarendon Press; 1990.
- Singh K, Blümich B. NMR spectroscopy with compact instruments. *Trends Anal Chem.* 2016;83:12–26.
- Jones AC, Sanders AW, Bevan MJ, Reich HJ. Reactivity of individual organolithium aggregates: a RINMR study of n-Butyllithium and 2-Methoxy-6-(methoxymethyl)phenyllithium. *J Am Chem Soc.* 2007;129(12):3492–3.
- Christianson MD, Tan EHP, Landis CR. Stopped-flow NMR: determining the kinetics of $[\text{rac}-(\text{C}_2\text{H}_4(1\text{-indenyl})_2)\text{ZrMe}][\text{MeB}(\text{C}_6\text{F}_5)_3]$ -catalyzed polymerization of 1-Hexene by direct observation. *J Am Chem Soc.* 2010;132(33):11461–3.
- Foley DA, Wang J, Maranzano B, Zell MT, Marquez BL, Xiang Y, et al. Online NMR and HPLC as a reaction monitoring platform for pharmaceutical process development. *Anal Chem.* 2013;85:8928–32.
- Clegg IM, Gordon CM, Smith DS, Alzaga R, Codina A. NMR reaction monitoring during the development of an active pharmaceutical ingredient. *Anal Methods.* 2012;4:1498–506.
- Foley DA, Bez E, Codina A, Colson KL, Fey M, Krull R, et al. NMR flow tube for online NMR reaction monitoring. *Anal Chem.* 2014;86(24):12008–13.
- Hall AMR, Chouler JC, Codina A, Gierth PT, Lowe JP, Hinternair U. Practical aspects of real-time reaction monitoring using multi-nuclear high resolution flowNMR spectroscopy. *Catal Sci Tech.* 2016;6:8406–17.
- Maiwald M, Fischer HH, Kim YK, Albert K, Hasse H. Quantitative high-resolution on-line NMR spectroscopy in reaction and process monitoring. *J Magn Reson.* 2004;166(2):135–46.
- Blümich B, Haber-Pohlmeier S, Zia W. *Compact NMR.* Berlin: de Gruyter; 2014.
- Zalasskiy SS, Danieli E, Blumich B, Ananikov VP. Miniaturization of NMR systems: desktop spectrometers, microcoil spectroscopy, and “NMR on a chip” for chemistry, biochemistry, and industry. *Chem Rev.* 2014;114:5641–94.
- Meyer K, Kern S, Zientek N, Guthausen G, Maiwald M. Process control with compact NMR. *Trends Anal Chem.* 2016;83:39–52.
- Blümich B. Introduction to compact NMR: a review of methods. *Trends Anal Chem.* 2016;83:2–11.
- McNair HM, Miller JM. *Basic gas chromatography.* New York: John Wiley & Sons, INC.; 1998.
- Wang Y, Jiang D, Dai L. Novel bronsted acidic ionic liquids based on benzimidazolium cation: synthesis and catalyzed acetalization of aromatic aldehydes with diols. *Catal Commun.* 2008;9(15):2475–80.
- Leonard NM, Oswald MC, Freiberg DA, Nattier BA, Smith RC, Mohan RS. A simple and versatile method for the synthesis of acetals from aldehydes and ketones using bismuth triflate. *J Org Chem.* 2002;67(15):5202–7.
- Küçük HB, Yusufoglu A, Mataracı E, Dösler S. Synthesis and biological activity of new 1,3-dioxolanes as potential antibacterial and antifungal compounds. *Molecules.* 2011;16(8):6806–15.
- Agirre I, Barrio VL, Guemez MB, Cambra JF, Arias PL. Acetals as possible diesel additives. In: Dos Santos Bernardes MA, editor. *Economic effects of Biofuel production.* In Tech. 2011. www.intechopen.com/books/economic-effects-of-biofuel-production/acetals-as-possible-diesel-additives. Accessed 27 Sep 2017.
- Bailey WF, Zarcone LMJ, Rivera AD. Selective protection of 1,2- and 1,3-diols via acylative cleavage of cyclic formals. *J Org Chem.* 1995;60:2532–6.
- Gaina L, Gal E, Mataranga-Popa L, Porumb D, Nicolescu A, Cristea C, et al. Synthesis, structural investigations, and DFT calculations on novel 3-(1,3-dioxan-2-yl)-10-methyl-10H-phenothiazine derivatives with fluorescence properties. *Tetrahedron Lett.* 2012;68:2465–70.
- Lidstrom P, Tierney J, Wathey B, Westman J. Microwave assisted organic synthesis. *Tetrahedron.* 2001;57:9225–83.
- Chen L, Nohair B, Kaliaguine S. Glycerol acetalization with formaldehyde using water-tolerant solid acids. *Appl Catal A Gen.* 2016;509:143–52.
- Guemez MB, Requies J, Agirre I, Arias PL, Barrio VL, Cambra JF. Acetalization reaction between glycerol and n-butyraldehyde using an acidic exchange resin. Kinetic modelling. *Chem Eng J.* 2013;228:300–7.
- Hong X, Mcgiveron O, Kolah AK, Orjuela A, Peereboom L, Lira CT, et al. Reaction kinetics of glycerol acetal formation via transacetalization with 1,1-diethoxyethane. *Chem Eng J.* 2013;222:374–81.
- Dalitz F, Kreckel L, Maiwald M, Guthausen G. Quantitative medium-resolution NMR spectroscopy under non-equilibrium

- conditions, studied on the example of an esterification reaction. *Appl Magn Reson*. 2014;45(5):411–25.
26. Zientek N, Laurain C, Meyer K, Kraume M, Guthausen G, Maiwald M. Simultaneous ^{19}F - ^1H medium resolution NMR spectroscopy for online reaction monitoring. *J Mag Reson*. 2014;249: 53–62.
 27. Agirre A, Garcia I, Reques J, Barrio VL, Guemez MB, Cambra JF, et al. Glycerol acetals, kinetic study of the reaction between glycerol and formaldehyde. *Biomass Bioenergy*. 2011;35:3636–42.
 28. Chopade SP, Sharma MM. Acetalization of ethylene glycol with formaldehyde using cation-exchange resins as catalysts: batch versus reactive distillation. *React Funct Polym*. 1997;34(1):37–45.